Audio Engineering Society

Convention Paper

Presented at the 143rd Convention
2017 October 18–21, New York, NY, USA

Interpolation and Display of Microphone Directivity Measurements using higher-order Spherical Harmonics

Jonathan D. Ziegler[1,3], Mark Rau[2], Andreas Schilling[3], and Andreas Koch[1]

[1]*Stuttgart Media University, Institute for Electronic Media, Stuttgart, Germany*
[2]*Stanford University, CCRMA, Department of Music, Stanford, CA, USA*
[3]*Eberhard Karls University Tübingen, Visual Computing, Tübingen, Germany*

Correspondence should be addressed to Jonathan D. Ziegler (zieglerj@hdm-stuttgart.de)

ABSTRACT

The accurate display of frequency dependent polar response data of microphones has largely relied on the use of a defined set of test frequencies and a simple overlay of two-dimensional plots. In recent work, a novel approach to digital displays without fixed frequency points was introduced. Building on this, an enhanced interpolation algorithm is presented, using higher-order spherical harmonics for angular interpolation. The presented approach is compared to conventional interpolation methods in terms of computational cost and accuracy. In addition, a three-dimensional data processing prototype for the creation of interactive, frequency-dependent, three-dimensional microphone directivity plots is presented.

1 Introduction

Traditional displays of directional microphone sensitivity provide a limited insight into the frequency-dependent directivity characteristics. The use of defined test frequencies, multiple measurement overlays, and the restriction to two dimensions reduces the amount of information that can be obtained from such figures. As an improvement, the authors suggested a software-based display with a non-fixed frequency point. Using this, an interactive display of the directivity properties of microphones and coincident arrays can be created [1]. One crucial element of data processing for this application is the angular interpolation. This paper focuses on the use of spherical harmonic interpolation (SHI) for this task. Both speed and accuracy are compared to the performance of traditional 3^{rd}- order spline interpolation. In an evaluation using measured data, depending on the order of SHI, the interpolation speed and accuracy outperformed traditional spline interpolation. In addition, the simplicity of adaptation to three-dimensional measurements is shown on simulated measurement data.

2 Methods

2.1 Cubic Spline Interpolation

The angular resolution of measurement data can be increased by creating virtual measurement points. This

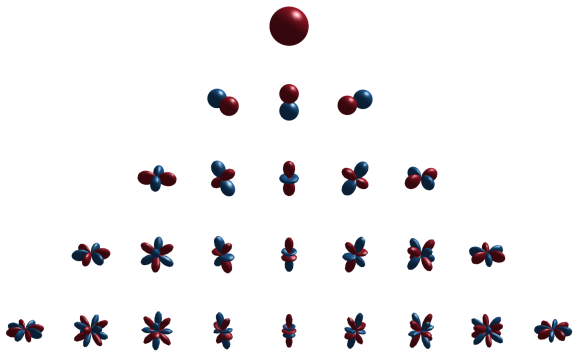

Fig. 1: Spherical harmonics with $n \leq 4$. Only components relevant to the xy plane are used for two-dimensional interpolation.

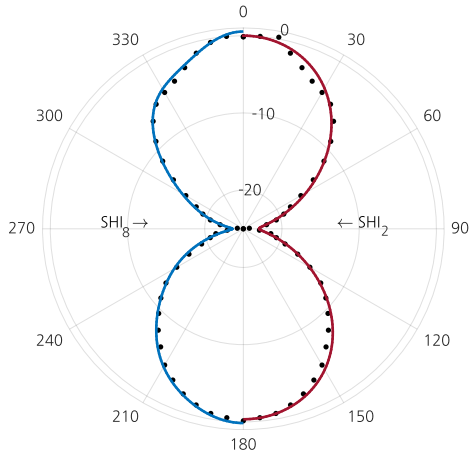

Fig. 2: Comparison of spherical harmonic interpolation computed with order limits of 2 and 8. While $n \leq 2$ provides a smoother angular response, $n \leq 8$ retains a higher level of detail. Measurement data: Schoeps MK8 at 10 kHz

was formerly achieved using cubic spline interpolation, which uses third order polynomials within every interval between measurement points $[S_i(\nu), S_{i+1}(\nu)]$ with $i = 0, 1 \ldots$ [2, 3].

Considering the i^{th} spline interval S_i, the interpolation function takes the form:

$$S_i(\tau) = a_i + b_i\,\tau + c_i\,\tau^2 + d_i\,\tau^3 \tag{1}$$

with $0 \leq \tau \leq 1$. By defining a set of boundary conditions appropriate to the system's physical behavior, it is possible to solve for all variables a_i, b_i, c_i and d_i in every interval i and at all frequencies ν.

2.2 Spherical Harmonic Interpolation (SHI)

A more elegant approach uses spherical harmonics for this task. This set of orthogonal base functions defined on the surface of a sphere can be expressed as

$$Y_n^m(\theta,\phi) = \sqrt{\frac{2n+1}{4\pi}\frac{(n-m)!}{(n+m)!}}P_n^m(\cos\theta)e^{im\phi}, \tag{2}$$

where $P_n^m(\cdot)$ are the associated Legendre functions, m is an integer representing the function degree, and n is a natural number representing the function order [4]. The associated Legendre functions are derived by differentiating the Legendre polynomials and are given as

$$P_n^m(x) = (-1)^m(1-x^2)^{m/2}\frac{d^m}{dx^m}P_n(x),\ x \in [-1,1], \tag{3}$$

with $P_n(x)$ representing the Legendre polynomials which arise when $m = 0$. They are defined as

$$P_n(x) = \frac{1}{2^n n!}\frac{d^n}{dx^n}(x^2-1)^n. \tag{4}$$

Spherical harmonics have the useful property that any arbitrary function on a sphere $f(\theta,\phi)$ can be be represented as

$$f(\theta,\phi) = \sum_{n=0}^{\infty}\sum_{m=-n}^{n} f_{nm}Y_n^m(\theta,\phi), \tag{5}$$

with f_{nm} being the function weights defined as

$$f_{nm} = \int_0^{2\pi}\int_0^{\pi} f(\theta,\phi)[Y_n^m(\theta,\phi)]^* \sin\theta d\theta d\phi. \tag{6}$$

The weights form what is known as the spherical Fourier transform, while equation (5) is the inverse spherical Fourier transform [4, 5].

Using equations 5 and 6, a spherical harmonic data interpolation method can be devised. Measurement data are transformed via spherical Fourier transform

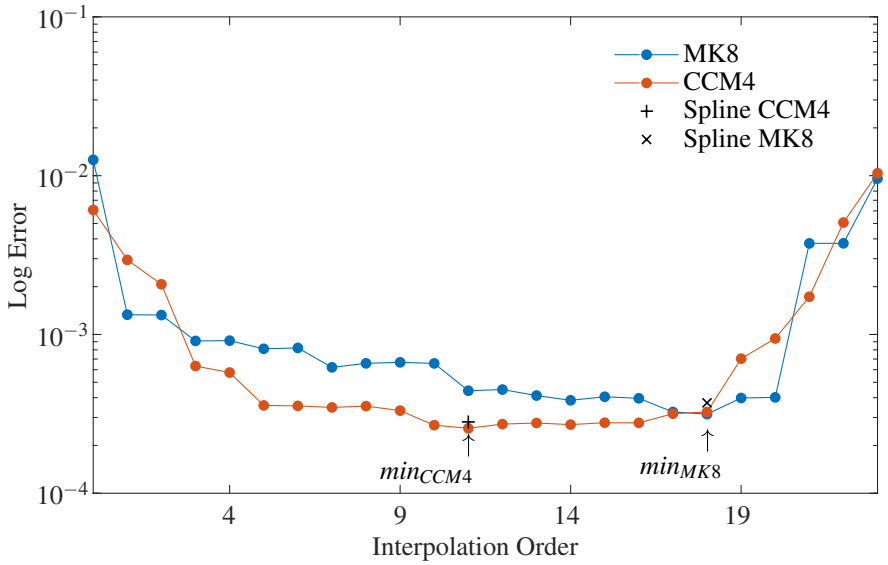

Fig. 3: Comparison of algorithm accuracy. Interpolated measurement points from a down-sampled dataset are compared to high-resolution measurements. The error is computed as the sum of absolute errors over 72 points on 360°. Due to the small change in error over a large range of SHI orders, a logarithmic display is chosen. At the indicated minima, SHI outperforms cubic spline interpolation by approximately 0.25 dB for the Schoeps CCM4 cardioid capsule and by approximately 0.5 dB for the Schoeps MK8 figure-of-eight capsule used for the measurements.

onto a base of spherical harmonic functions $Y_n^m(\theta_j, \phi_k)$, sampled on a grid of dimension $j \times k$, matching the resolution of the measurement data. Later, an inverse spherical Fourier transform onto a grid with a higher spatial resolution results in the desired discrete angular interpolation. Since the spherical harmonic base functions are continuous, the discrete resolution of the interpolated data depends on the grid for the inverse spherical Fourier transform and therefore can be varied.

3 Results

The use of spherical Fourier transforms for data interpolation creates an effective approach to angular smoothing within the application described in section 4. Lower-order transforms provide the capability to retrieve the basic microphone directivity characteristics with computational efficiency, while higher-order transforms outperform the traditional spline methods in terms of accuracy.

All basic microphone polar patterns inherent to pressure sensors and pressure-gradient sensors can be described using an omnidirectional sphere and a bidirectional

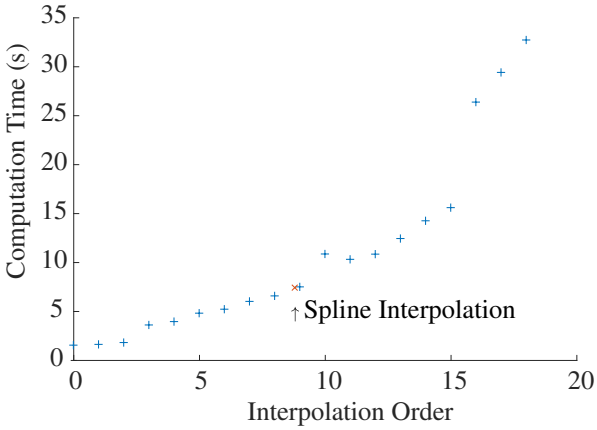

Fig. 4: Computational cost of interpolation algorithms. 24 Measurement points with 20000 frequency bins each were processed. Up to $n = 8$, spherical harmonic interpolation is faster than spline interpolation.

figure-of-eight [6, chapter 5]. Hence, combinations of spherical harmonics with $n \leq 1$ are sufficient. Adding higher order spherical harmonics subsequently adds additional information about the measured microphone response. Figure 1 shows the first 5 orders of spherical harmonics ($0 \leq n \leq 4$). It is apparent that $n = 0$ is analogous to omnidirectional microphone characteristics, while $n = 1$ produces functions in clear relation to figure-of-eight microphone polar patterns with orthogonal spatial orientation.

Figure 2 shows data interpolation using spherical harmonics with $n \leq 2$ and $n \leq 8$. The measurements were performed on a Schoeps MK8 figure-of-eight capsule sampled at 37 points between 0° and 180° along the horizontal plane, resulting in an angular resolution of 5°. For ease of display and assuming rotational symmetry in the MK8's polar pattern, the 180° measurement was expanded to a full circle.

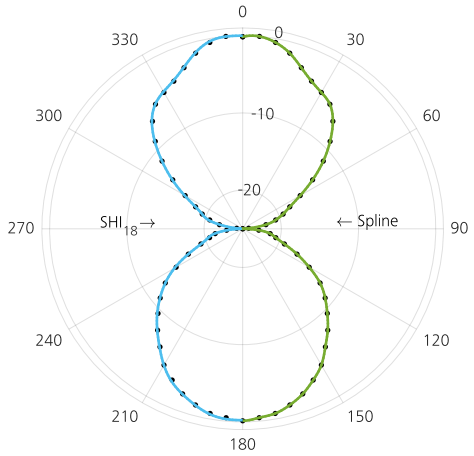

Fig. 5: Comparison of higher-order ($n \leq 18$) spherical harmonic interpolation and cubic spline interpolation.

3.1 Performance

The proposed algorithms are currently computed within Mathworks' Matlab®, using the AKtools toolbox [7]. With this setup, the processing time for data interpolation was inspected on a dataset with 24 measurement points ($\Delta\theta = 15°$) and 20000 frequency bins. Figure 4 shows that for the presented case, spherical harmonic interpolation provides faster results than spline interpolation up to an order of $n = 8$.

3.2 Accuracy

To compare the quality of interpolated data, a set of measurements was down-sampled by a factor of 3, going from $\Delta\theta = 5°$ to $\Delta\theta = 15°$. After data interpolation, the difference between interpolated data points and actual omitted measurement points was calculated. Figure 3 shows the resulting error values for different orders of spherical harmonic interpolation, compared to the error of spline interpolation. Both cardioid and figure-of-eight characteristics can be interpolated to a high level of accuracy with surprisingly low orders of interpolation. Taking the logarithmic nature of Figure 3 into account, acceptable results are achieved with orders as low as 3. This is in part due to the very rough sampling of only 24 points. Figures 2 and 5 show that with higher measurement resolution, higher order interpolation is advisable. Figure 3 also shows that, assuming maximum-order SHI as defined in section 3.3, cubic spline interpolation is outperformed by spherical harmonic interpolation. For the CCM4 capsule, SHI at 10 kHz results in approximately 0.25 dB less total error, for the MK8 capsule, the difference amounts to approximately 0.5 dB.

3.3 Aliasing

There are multiple ways to sample points on a sphere but the choice is often dependent on the measurement apparatus. Two common methods are Equal Angle Sampling which samples a sphere at uniformly-spaced angular positions, and Gaussian Sampling which samples the sphere with evenly spaced angles along the sphere [4]. Equal Angle Sampling requires $4(n+1)^2$ samples, where n is the desired order of spherical harmonics, while Gaussian Sampling only requires $2(n+1)^2$ samples. This study uses equal sampling along the azimuthal angle, so Gaussian sampling is used and $2(n+1)$ equal-angle samples are required along the azimuthal angle. Originally, measurements were taken at 5° along the azimuth. After extrapolation to 360° and the removal of duplicate measurement locations at 0° / 360° and 180°, 72 measurement points remain, resulting in a maximum spherical harmonic order of $n = 35$. When the data are down-sampled to 15° angles for verification, the maximum spherical harmonic order becomes $n = 11$. If interpolation is performed at a higher order than the maximum order defined by the sampling rate, aliasing can occur. An example of possible aliasing is shown in Figure 6.

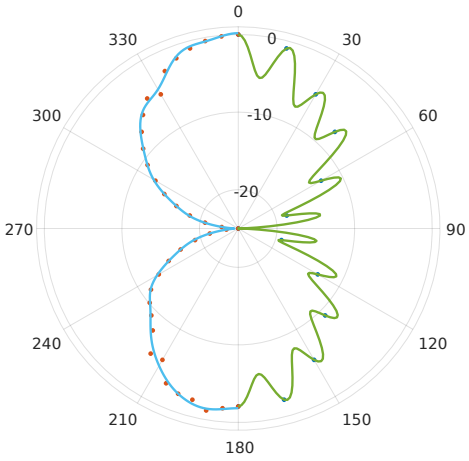

Fig. 6: Aliasing effects due to interpolation above the sampling limit. *Left:* Dataset with 72 measurement points in 360°, interpolated with $n \leq 23$. *Right:* Dataset with 24 measurement points in 360°, interpolated with $n \leq 23$. Choosing interpolation orders above the sampling limit introduces unwanted oscillations in the interpolated data. The higher the order, the more drastic the oscillations.

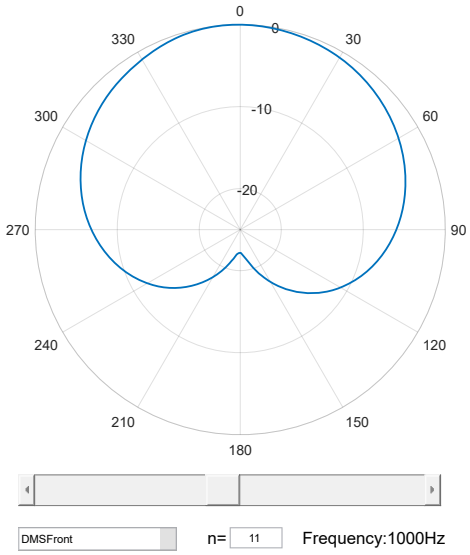

Fig. 7: Example application for SHI methods. Software prototype interactively displaying frequency dependent microphone polar data with variable angular smoothing.

4 Application

Currently the primary use for the developed approach is within a software prototype for the interactive display of frequency dependent microphone polar patterns [1]. Building on this prototype, spherical harmonic interpolation enables the user to adjust the amount of angular smoothing applied to the data. Figure 7 shows measurement data of a Schoeps CCM4 cardioid capsule being displayed at 1000 Hz with an interpolation order of 11. The original measurements were gathered with an angular resolution of 15°, therefore $n \leq 11$ is the highest order of interpolation below the aliasing threshold. Expanding the software to three-dimensional balloon plots is easily achieved by expanding the grids for the spherical Fourier transform and the inverse transform to a 3-D system. This is discussed in the following section. The multidimensional display of transducer measurement data is common practice for loudspeaker measurements and can be achieved using various approaches, with contour and balloon plots being the most prominent [8, 9]. In the context of microphone characterization, this is less common.

5 Outlook

As described by Angus and Evans [10], SHI can be used to interpolate three dimensional measurements of transducer behavior. Lacking sufficient measurement data, the two-dimensional set used for Figures 2, 5, and 6 was extrapolated to a three-dimensional system. Added noise was applied to create a dataset with imperfect rotational symmetry. Figure 8 shows the raw data, alongside interpolations using $n \leq 7$ and $n \leq 17$. Future investigations will be focused on the acquisition and processing of three dimensional microphone characteristics.

6 Summary

In the context of an interactive method for the frequency-dependent display of microphone directivity measurements, spherical harmonic interpolation is introduced. The computational cost of the operation is compared to that of the more traditional and less application-specific approach of cubic spline interpolation. Within the used environment, SHI can be shown to be the faster processing method when interpolating at lower orders. In addition, the accuracy of the mentioned interpolation methods are compared by

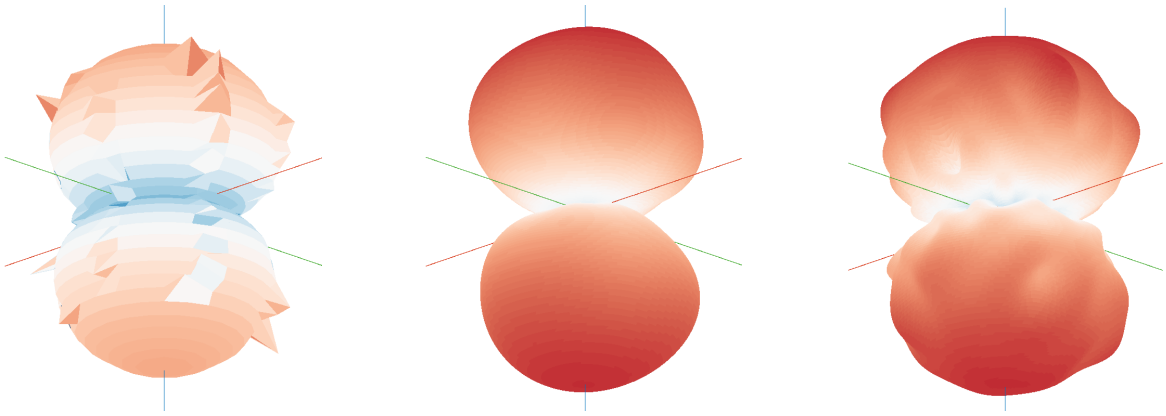

Fig. 8: Three-dimensional SHI demonstrated on simulated measurement data. The planar measurement of a Schoeps MK8 figure-of-eight capsule is expanded, making use of the inherent rotational symmetry of such microphones. Later, this symmetry is partially broken by randomly scaling some of the impulse responses using a normal distribution with $\mu = 1, \sigma = 0.5$. This synthesized dataset is interpolated using SHI_7 and SHI_{17}.

omitting data from a measurement and comparing the algorithmically synthesized data with actual measurements. Based on this comparison, it is possible to show that SHI outperforms cubic spline interpolation when the interpolation order is chosen close to the aliasing limit described in section 3.3. As a proof of principle, three-dimensional SHI for microphone patterns is demonstrated on a semi-synthesized dataset consisting of planar measurement data and noise.

References

[1] Ziegler, J. D., Paukert, H., and Runow, B., "Interactive Display of Microphone Polarity Patterns with Non-Fixed Frequency Point," in *Audio Engineering Society Convention 142*, 2017.

[2] Bartels, R. H., Beatty, J. C., and Barsky, B. A., *An Introduction to Splines for Use in Computer Graphics and Geometric Modeling (The Morgan Kaufmann Series in Computer Graphics)*, Morgan Kaufmann Pub, 1987, ISBN 0934613273.

[3] Weisstein, E. W., "Cubic Spline." *MathWorld – A Wolfram Web Resource*, 2017.

[4] Rafaely, B., *Fundamentals of spherical array processing*, volume 8, Springer, 2015.

[5] Williams, E. G., *Fourier acoustics: sound radiation and nearfield acoustical holography*, Academic press, 1999.

[6] Eargle, J., *Eargle's The Microphone Book: From Mono to Stereo to Surround - A Guide to Microphone Design and Application (Audio Engineering Society Presents)*, Focal Press, 2004, ISBN 0240519612.

[7] Brinkmann, F. and Weinzierl, S., "AKtools - An Open Software Toolbox for Signal Acquisition, Processing, and Inspection in Acoustics," in *Audio Engineering Society Convention 142*, 2017.

[8] Sridhar, R., Tylka, J. G., and Choueiri, E., "Metrics for Constant Directivity," in *Audio Engineering Society Convention 140*, 2016.

[9] Klippel, W. and Bellmann, C., "Holographic Nearfield Measurement of Loudspeaker Directivity," in *Audio Engineering Society Convention 141*, 2016.

[10] Angus, J. A. S. and Evans, M. J., "Polar Pattern Measurement and Representation with Surface Spherical Harmonics," in *Audio Engineering Society Convention 104*, 1998.